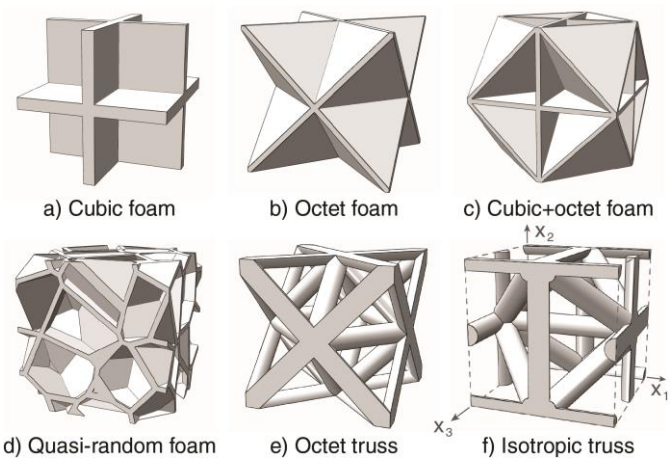

Figure 1 | Material geometries. Representative topologies of six cellular structures studied, all with solid volume fractions, $(\bar{\rho}/\rho_S) = 0.2$. A coordinate system aligned with the axes oriented in the cubic directions is shown for the isotropic truss. This coordinate system is used in the cubic orientation for all systems depicted in this figure and is utilized to define the Young's and shear modulus and the Poisson ratio for the materials.

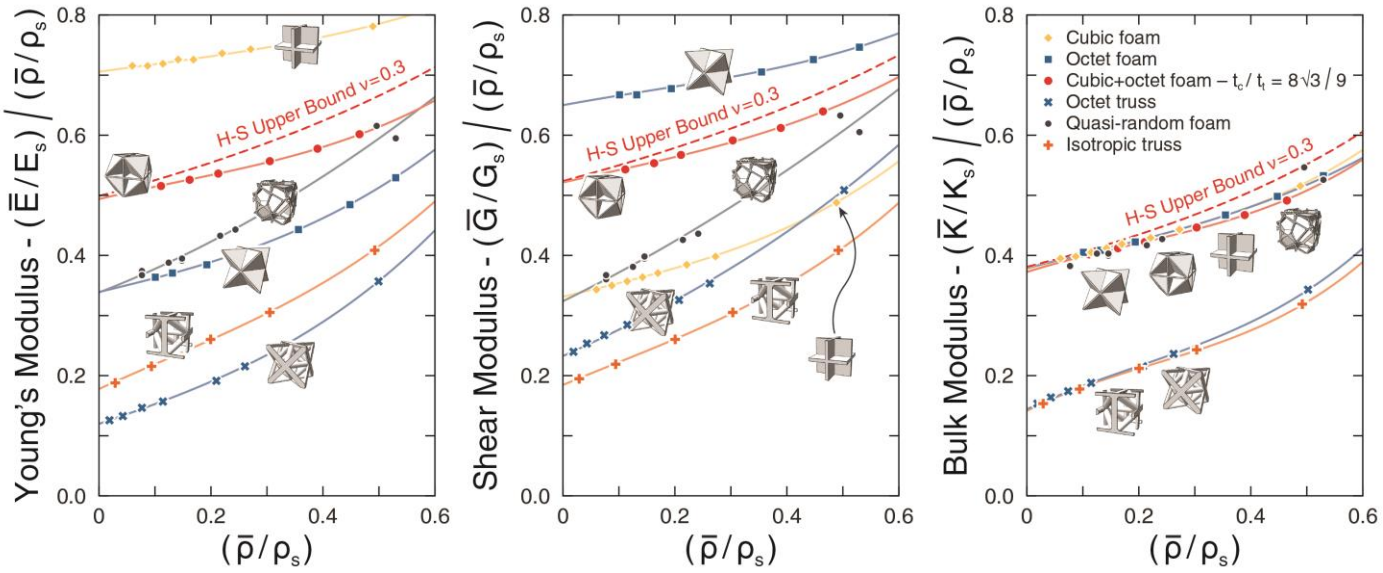

Figure 2 | Young's, shear and bulk modulus. The elastic stiffness of six material geometries, characterized by E, G, and K, the Young's shear and bulk modulus respectively. The Hashin-Shtrikman theoretical upper bounds for isotropic stiffness are plotted for each modulus. Only anisotropic materials can have stiffnesses in excess of the upper bounds. Open cell materials underperform closed cell materials by a large margin.

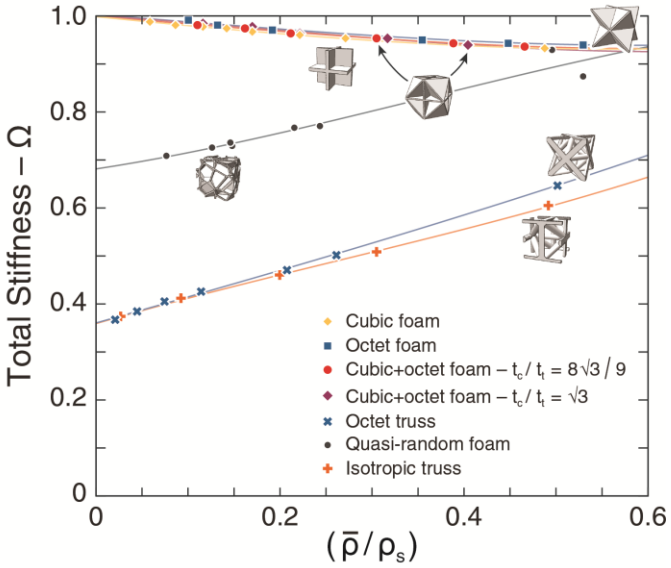

Figure 3 | Total stiffness. Structural performance in terms of elastic strain energy storage. A material that achieves the theoretical upper bound will have $\Omega \to 1$ as $(\bar{\rho}/\rho_S) \to 0$. Materials can achieve the bounds at low relative densities when stress and strain energy concentrations are limited to very small regions near cell edges. As relative density increases and members become thicker, non-uniformities become significant and an inability to achieve the theoretical bounds is observed, although, further optimization may be possible. There are three classes of material performance: maximally stiff closed cell materials, closed cell materials with geometric features that allow for bending, and ordered maximally stiff open cell materials.

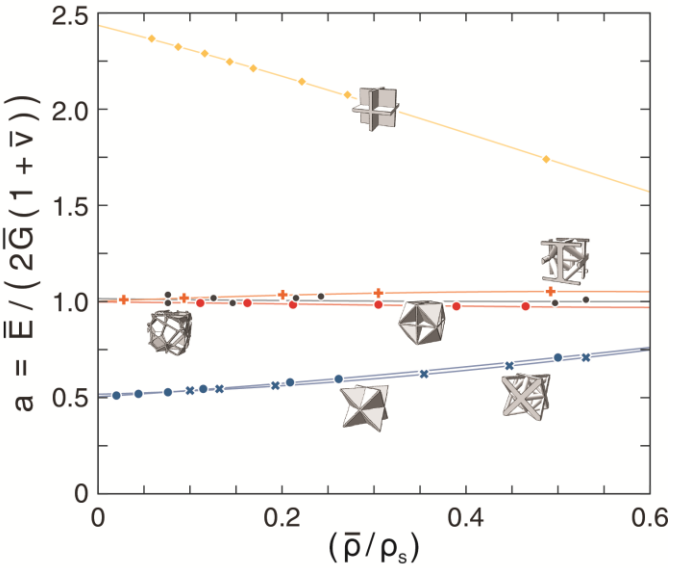

Figure 4 | The Zener anisotropy ratio. Both the cubic+octet foam with $t_c/t_t = 8\sqrt{3}/9$ and the isotropic truss have $a \to 1$ as $(\bar{\rho}/\rho_S) \to 0$. The octet-foam and –truss both have nearly identical values of a, while the cubic foam is the most anisotropic. The anisotropy of the cubic+octet foam can be tailored by adjusting the ratio of wall thicknesses, t_c/t_t, where t_c and t_t are the wall thicknesses of the cubic and octet foam subgeometries respectively. For example, with $t_c/t_t = \sqrt{3}$ isotropy is achieved at $(\bar{\rho}/\rho_S) = 40\%$.

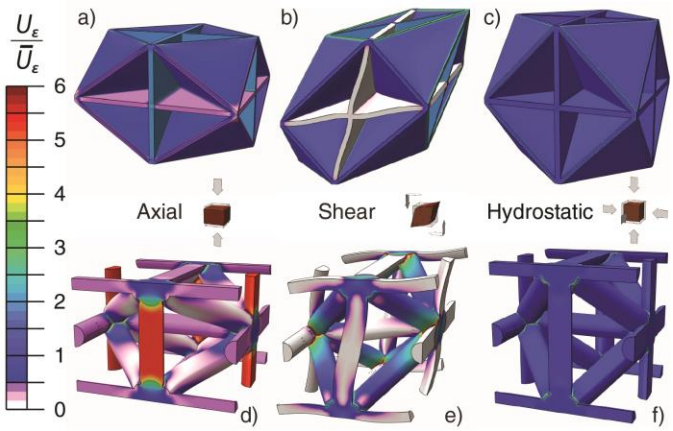

Figure 5 | Strain energy distributions. Axial (a and d), shear (b and e), and hydrostatic strain (c and f), in the cubic+octet foam (top row) and isotropic truss (bottom row). The local strain energy density, U_ε, is normalized by the macroscopic solid fraction strain energy density, $\bar{U}_\varepsilon$. The imposed strains are small, but exaggerated to reveal their nature. Both geometries have, $(\bar{\rho}/\rho_S) = 0.2$.

Methods:

To assess geometric efficiency, we use a representative volume element (RVE) finite element (FE) modeling technique. Periodic boundary conditions (BC) allow us to model states of homogeneous macroscopic strain. Load states are imposed by prescribing the displacements of "virtual" nodes, and the principle of virtual work is used to calculate the stresses[28]. The details of this method are described by *Danielsson, Parks and Boyce*[28]. We report the Cauchy stress, which is equivalent to the First Piola-Kirchhoff stress when strains are small. Moduli are calculated through application of states of macroscopic strains consistent with states of uniaxial stress, pure shear, and pure dilatation (illustrated in FIGs.E1, E2, E3, respectively); here the coordinate axes are aligned with the edges of the cubic unit cells (**FIG.2**)

The commercial FE code Abaqus CAE[25] is used to generate model geometries and evaluate FE model solutions. Quadratic elements, fully integrated tetrahedral elements with ten nodes (C3D10) and 20-node brick elements (C3D20) are used. The imposed strains are small, however, nonlinear deformations are allowed using the *nlgeom* flag in Abaqus. The accuracy of the finite element (FE) method was assessed through direct comparison with experimental data, the predictions of analytical models, basic structural analysis, and against a more thorough study involving similar quasi-random closed cell foams[32] (see S.3).

As metrics for performance we use a suite of theoretical bounds, for Young's, shear and bulk modulus, developed by Hashin and Shtrikman[14] (H-S). The H-S bounds govern the stiffness of nearly isotropic multiphase materials. It is applied to foams and lattices by setting one of the phases in a two-phase system to have zero stiffness. The bounds then simplify to[11]:

$$\frac{K_{HSU}}{K_s} = \frac{4G_s(\bar{\rho}/\rho_s)}{4G_s+3K_s(1-\bar{\rho}/\rho_s)}, \tag{3}$$

$$\frac{G_{HSU}}{G_s} = \frac{(9K_s+8G_s)(\bar{\rho}/\rho_s)}{20G_s+15K_s-6(K_s+2G_s)(\bar{\rho}/\rho_s)} \tag{4}$$

The bound on Young's modulus is found by the application of isotropic linear elasticity on the preceding bounds to get,

$$E_{HSU} = \frac{9G_{HSU}K_{HSU}}{3K_{HSU}+G_{HSU}}, \tag{5}$$

where the subscript *HSU* denotes the H-S upper bound, the subscript *s* denotes the property of the constituent, and *E*, *G*, and *K*, are the Young's, shear, and bulk modulus respectively. The corresponding Poisson ratio is,

$$\nu_{HSU} = \frac{3K_{HSU}-2G_{HSU}}{2(3K_{HSU}+G_{HSU})}, \tag{6}$$

Quasi-random closed cell geometries are generated using Voronoi tessellation. A hard sphere seeding model is used to control the spacing between seed points and the resulting distribution in cell sizes. The sphere diameter is,

$$d = 2\alpha\left(\frac{3}{4\pi n}\right)^{1/3}, \tag{7}$$

where $\alpha = 0.55 - 0.6$ is the packing density of the hard spheres, and n is the number of unique cells in a unit cell. The initial seed is placed in the corner of a cubic RVE, this helps to insure the continuity of material in the unit cell geometry. Seed points are added randomly to the RVE. If a new seed causes overlap of the hard spheres it is removed and another attempt is made. If a maximum number of attempts is made in a single step the entire process is reinitialized and repeated until a solution is reached.

Macroscopic strains consistent with states of axial, shear and hydrostatic stress are applied to calculate the nine independent elastic constants for an orthotropic material. These are then averaged to calculate $\bar{E}$, $\bar{G}$ and $\bar{K}$. For cubically symmetric geometries only three elastic constants need to be calculated.

Input into our design scheme was in the form of material geometries taken from the literature. Geometries such as the body centered cubic (BCC) Kelvin foam[33], a similar geometry based instead on the spatial tessellation of space from the face centered cubic (FCC) seeding of space, the cubic foam, the octet-foam, as well as a variety of others, most of which have been omitted for the sake of brevity and clarity, were assessed using the analytical scheme provided in this work. Through inspection, we are able to identify the morphological features associated with high performance. It is through the identification and combination of fundamental geometries, in a genetic-type scheme, that we are able to produce novel geometries with extremal properties.

Data Availability:

Source data for finite element results in figures [2-5, and ED5] are provided with the paper.

Additional References:

32. Roberts, a. P. & Garboczi, E. J. Elastic moduli of model random three-dimensional closed-cell cellular solids. *Acta Mater.* **49,** 189–197 (2001).

33. Thomson, S. W. On the Division of Space with Minimum Partitional Area. *Acta Math.* **11,** 121–134 (1888).